One-step formation of ZrON thin film on surface of carbon fine particles for membrane electrode assembly

Yudai Aihara, Takashi Iida, Kakeru Kodama, Hiroshi Iwata, and Takao Sekiya[a]

Yokohama National University, 79-5 Tokiwadai, Hodogaya-ku, Yokohama 240-8501 Japan

[a] Electronic mail: sekiya-takao-jx@ynu.ac.jp

Abstract

Zirconium nitrides and oxynitride films were deposited on alumina or carbon particles by reactive sputtering using a magnetron sputtering apparatus with a Zr hollow cylindrical target and a vibrating equipment with heating capability. The vibrating equipment developed in this study was effective if the particles are spherical and highly monodisperse. Uniform film deposition was achieved over the entire surface of highly monodisperse spherical alumina particles using the vibrating equipment during deposition. Pure ZrN crystalline layers was deposited under Ar and N_2 gas flows with heating on XC-72 carbon powder particles removed adsorbed oxygen. EDS mapping analysis for deposited XC-72 carbon particles showed ubiquitous film deposition on agglomerated particles regardless of the vibration during sputtering. Uniform film deposition with vibrating equipment was achieved on the entire surface of CGB-10 particles with more spherical and monodisperse than XC-72 but precipitated crystalline phase depended on unintentional oxygen chemisorbed on the particles. Addition and increase in flow rate of oxygen to the sputtering gas resulted in the formation of desired crystalline phase, Zr_2ON_2, $Zr_7O_8N_4$ and monoclinic ZrO_2, precipitated in the film using CGB-10 particles with chemisorbed oxygen removed. Current density for oxygen reduction reaction measured for MEA made from CGB-10 particles with ZrON-based crystals deposited was larger than that for thin film deposited on carbon plate substrate.

I. INTRODUCTION

Fuel cells, which produce only water from oxygen and hydrogen in an ideal reaction, are clean electrochemical energy conversion devices and have attracted considerable attention owing to their high energy conversion efficiency and low environmental load. With the practical application of fuel cells approaching reality toward a decarbonized and sustainable energy society, there are still some problems to be solved to spread them commonly. Fuel cells are classified according to the type of electrolyte used at temperatures at which the electrolyte exhibits sufficient and stable ionic conductivity. Solid polymer fuel cells (PEFC) in which a fluorine-based cation exchange membrane is used as the electrolyte with low operating temperatures has the potential to be widely applied to households and automobiles. The cation exchange membrane is brought into close contact with electrodes made from carbon-supported catalysts on both fuel and air sides. The assembly integrated with the cation exchange membrane and the electrode is called the membrane electrode assembly (MEA). Since the cation exchange membrane is highly acidic, the electrode catalyst material and constituent materials should have high corrosion resistance. Therefore, nowadays, platinum is currently and commonly used as the electrode catalyst material in PEFCs.[1] There are two major problems on the use of platinum as an electrode catalyst: high procurement cost and limited of recoverable reserves.[2] To solve these problems, it is necessary to develop an electrode catalyst material that can replace platinum, and many studies have been performed on catalysts with Fe-N-C,[3-5] Hf,[6,7] Pd-Co,[8] Ta,[9,10] Ba,[11] Ti [12] and polyaniline-Fe, Co.[13]

On the other hand, many studies have been performed on the application of zirconium oxynitride (ZrON) for an electrode catalyst material in PEFCs as an alternative to platinum catalyst.[14-20] It has been shown that the oxygen reduction potential of ZrON is high depending on its synthesis conditions.[14] Zirconium is inexpensive, relatively high abundant in the Earth's crust, and has high acidic resistance, so that the use of ZrON as an electrode catalyst material is one of the best options. Many research studies on the synthesis of ZrON on several planar substrates and on its catalytic properties were performed because its use as a catalyst has attracted considerable attention.[18-21] As a composite catalyst in MEA, it is necessary to form ZrON film on the surface of carbon fine particles instead of the platinum composite catalyst.[14,15,17] The preparation of an electrocatalyst involves two steps: the preparation of the precursor of zirconium oxide on carbon particles and the pyrolysis of the zirconium oxide in an atmosphere of gaseous NH_3.[14,15] A wet process is used for the formation of the precursor in which zirconium oxide is uniformly dispersed on the particle surface.[15]

As a new one-step preparation method for the catalyst in MEA, we directly deposited catalysts on the surface of carbon particles by magnetron sputtering which is widely used in industry.[20] The magnetron sputtering apparatus with a hollow cylindrical Zr target developed in our laboratory enables the films to be deposited from various directions owing to the inner erosion of the hollow cylindrical target. We developed a new vibrating equipment with heating capability to shake powder particles to deposit films on all the surfaces of the particles. The heating of the powder enables the deposition of well-crystallized ZrON films on the surfaces of the particles reproducibly. Since the vibrating equipment makes the powder particles bounce and flip, the film deposition by

sputtering can be always performed on fresh surfaces of the particles. First, in this study, the performance of the vibrating equipment was evaluated by depositing ZrN film on highly monodisperse spherical alumina particles. Next, ZrON film is deposited on two kinds of carbon powder with different particle size using the vibrating equipment with heating capability and the obtained films were characterized by scanning electron microscope (SEM), energy dispersive X-ray spectroscopy (EDS), XPS, XRD and electrochemical measurement.

II. EXPERIMENTAL

To shake and heat substrate particles during spattering, we developed a vibrating equipment with heating capability, as shown in Fig. 1. An Inconel plate heater was fixed over a leaf spring with a permanent magnet. The Inconel heater has a circular depression 10 mm in diameter and 3 mm deep on which a small amount of powder can be placed. The electric current of an electromagnetic coil fixed on another leaf spring was operated by a function generator (IWATSU SG-4104), and the vibration of the leaf spring, thus obtained, was conducted to the heater where the substrate powder was placed in the depression. The Inconel heater is covered with an insulating film of ZrO_2 by sputtering, and the heater temperature was controlled up to ~750°C by adjusting the amount of heater current while checking the temperature with a radiation thermometer (LEC L-1000).
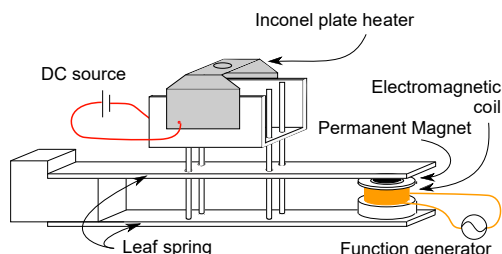
Fig.1 Vibrating equipment with having Inconel 625 plate heater with a circular recess of 10mm diameter.

The details of our sputtering apparatus are shown in a previous work.[21] The flow rates of sputtering gases were adjusted using mass flow controllers. The common sputtering conditions, the total pressure during the deposition, the deposition time and the discharge DC power provided by a sputtering power supply, TruPlasma DC3000 (TRUMPF Huettinger GmbH+Co) were 0.7 Pa, 60 min and 600 W, respectively. Experimental conditions for film deposition such as substrate particles, presence or absence of vibration, Inconel heater temperature during sputtering, etc. are summarized in Table 1. Spherical alumina (Alnabeads A40, Showa Denko), carbon black (VULCAN XC-72, Fuel Cell Store) and graphite powder (CGB-10, Nippon Graphite) were used as substrate particles. The pre-sputtering process to clean the target surface was performed under only Ar flow at a rate of 50 sccm for 60 min before film deposition with the shutters attached to both the upper and lower edges of the hollow cylindrical target closed. This pre-sputtering process also served as a getter pump in which the reaction of sputtered Zr with residual gases results in a higher vacuum pressure than the background pressure. XRD, XPS and SEM measurements for deposited carbon powders were performed using SmartLab (RIGAKU), Qunatera-SXM (ulvac PHI) and SU-8010 (Hitachi High-Tech), respectively.

5

Some MEAs were fabricated for electrochemical measurement from the sample particles with ZrON thin film. A solution of each sample particle mixed with 5 % Nafion dispersion solution and 99 % ethanol at a mass ratio of 1:9:90, was dropped onto the plastic formed carbon (PFC) substrate and spread over the entire surface of the substrate by spin-coating method. The MEA of each sample were prepared by heating them in a nitrogen atmosphere at 120°C for 1 hour. Cyclic voltammetry (CV) and slow scan voltammetry (SSV) for the sample MEAs were carried out in electrolyte of 0.1 M sulfuric acid by varying the potential of the working electrode which was the MEA itself from 1.0 to -0.15 V with a silver/silver chloride electrode and platinum plate as the reference and counter electrodes, respectively. Two types of working electrode potential dependence curves for current density at surface of MEA in contact with solution were recorded in an oxygen removed solution previously purged with nitrogen and in an oxygen dissolved solution purged with oxygen by SSV measurements. The change in current density owing to oxygen reduction reaction (ORR) was evaluated by substruction of the current density measured in the oxygen removed solution from that in the oxygen dissolved solution by the SSV measurement.

Table 1   Experimental conditions for depositing film on substrate particles: The column "vibration" implies whether vibration was applied to the particles during deposition. The column "Temperature" is heater temperature during deposition. Samples with Yes in the "Heating before Deposition" column were heated at 750°C for 1 hour before deposition. The column "Microwave" indicates whether removing oxygen adsorbed on the particle surface was performed by microwave irradiation at 500 W for 3 minutes. All samples were deposited under Ar and N_2 flow at rates of 50 and 40 sccm, respectively. In the Samples I to M, O_2 was also added during deposition, so the flow rate was listed in the column "O_2 flow rate".

Sample	substrate	Vibration	Temperature	Heating before deposition	microwave	O_2 flow rate
A	Sphere Alumina	No	Room Temp.	No	No	None
B	Sphere Alumina	Yes	Room Temp.	No	No	None

C	XC-72	No	Room Temp.	No	No	None
D	XC-72	No	750 °C	No	No	None
E	XC-72	No	750 °C	Yes	No	None
F	XC-72	Yes	750 °C	Yes	No	None
G	CGB-10	No	750 °C	Yes	No	None
H	CGB-10	Yes	750 °C	Yes	No	None
I	CGB-10	Yes	750 °C	Yes	Yes	0.0 sccm
J	CGB-10	Yes	750 °C	Yes	Yes	0.2 sccm
K	CGB-10	Yes	750 °C	Yes	Yes	0.4 sccm
L	CGB-10	Yes	750 °C	Yes	Yes	0.6 sccm
M	CGB-10	Yes	750 °C	Yes	Yes	0.8 sccm

III. RESULTS AND DISCUSSION

A. Film deposition on Spherical Alumina particles

In order to deposit ZrN thin film on spherical alumina fine particles, sputtering was performed with Ar and N_2 flow at a rate of 50 and 40 sccm, respectively. Sample A was formed under sputtering without vibration during deposition, while Sample B was formed with vibration. Figures 2(a) and (b) show SEM images of the sample A and sample B with the distribution of Zr and Al measured by EDS analysis. The spherical alumina fine particles shown in Figs 2 are spherical in shape, have excellent monodispersibility. Figure 2(a) indicates that the surface of the individual alumina particles was partially covered with deposited Zr. On the other hand, Fig. 2(b) indicates that entire surface of the particles was covered with deposited Zr. It was confirmed visually through the window of the chamber during film deposition that the particles were

rolling finely in the circular depression of the heater by vibration of the heater. The difference in Zr distribution observed in Figs. 2 indicates that the vibrating equipment developed in this study is effective to achieve uniform deposition to entire surface of the spherical fine particles.
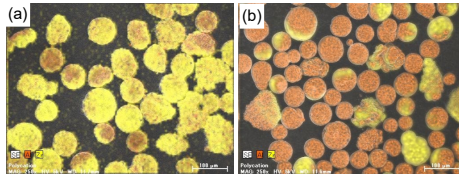
Figs.2 Zr and Al distribution measured by EDS of (a) sample A and (b) sample B.

B. Film deposition on XC-72 carbon particles

Samples C to F were deposited by sputtering with Ar flow at a rate of 50 sccm and N_2 flow at a rate of 40 sccm on XC-72 carbon powder. In the powder XRD diagrams of samples C to E and raw XC-72 powder shown in Fig. 3, two broad peaks observed at about 25° and 45° were originated from XC-72 carbon powder. Sample C deposited without heating has three small diffraction peaks at about 30.2°, 34.6° and 50.3°, which were assigned to tetragonal ZrO_2 (see Fig. 3). The small XRD diffraction intensities for Sample C suggested the presence of amorphous phase. It was shown that heating was required to sufficiently crystallize ZrON phase on the carbon powder particles. It was reported that the crystallized ZrN was precipitated at a heater temperature of 900 °C using a glassy carbon plate as the substrate[21] and that ZrN powder synthesized by ammonolysis of ZrO_2 was performed at temperature above 1200 ºC. [22] Sample D was deposited on XC-72 with Ar flow at a rate of 50 sccm and N_2 flow at a rate of 40 sccm

8

and the Inconel heater was heated to 750°C. The XRD diagram of sample D shown in Fig. 3 indicates the coexistence of diffraction peaks assigned to crystalline ZrN, monoclinic ZrO_2, and tetragonal ZrO_2. It should be considered that the carbon particle was heated by the heater to promote crystallization. This indicates that our Inconel heater has sufficient heating capability for the formation of well-crystallized ZrN or ZrO_2 with a little possibility of the coexistence of amorphous phases.[21,23] The presence of ZrO_2 or ZrON compounds in samples C and D, even though no oxygen gas was introduced, suggests unintended oxygen contamination during deposition. This phenomenon was caused by the higher reactivity of Zr with oxygen than with nitrogen. It was considered that this contamination of samples C, D was due to the desorption of oxygen adsorbed on the carbon powder introduced in the vacuum chamber and resulted in the formation of ZrO_2 or ZrON compounds. The increase in temperature of the carbon powder during deposition causes the desorption of adsorbed oxygen on the carbon powder, and a part of the desorbed oxygen atoms reacted with Zr. Therefore, it is necessary to remove such adsorbed oxygen from the carbon powder to deposit ZrN films of high purity. Sample E was deposited under the same conditions as sample D after baking XC-72 carbon powder at 750°C in vacuum for 1 hour to remove adsorbed oxygen. The XRD diagram of sample E shown in Fig. 3 indicates that no peaks assigned to ZrO_2 or ZrON compounds and diffraction peaks at 33.9° and 39.4° assigned to ZrN were observed. These indicate that baking before deposition was effective to remove adsorbed oxygen and that pure ZrN crystals could be formed on the surface of carbon particle. This knowledge is necessary for controlling the deposited phase by the oxygen flow rate.

9

The SEM image and EDS mapping of sample E shown in Figs. 4 shows that XC-72 particles were in various sizes due to aggregation and that deposited Zr was concentrated in some parts of the surface of aggregated particles. Figure 5 shows the SEM and EDS mapping images of sample F which was deposited under the same conditions as Sample E with applying vibration by the vibrating equipment. Comparing Figs. 4 and 5, there is little difference in Zr mapping between samples E and F, which were deposited without and with applying vibration, respectively. It is well known that carbon black particles generally agglomerate to form large secondary particles and are difficult to disperse with. It is assumed that the film formation being limited to secondary particles was due to the small size of the primary particles without agglomerated and their non-spherical shape, which prevented the vibrations from being transmitted to the particles resulting in poor movement of the particles. Shielding by the agglomerated secondary particles inhibited film deposition to primary particles during film formation.
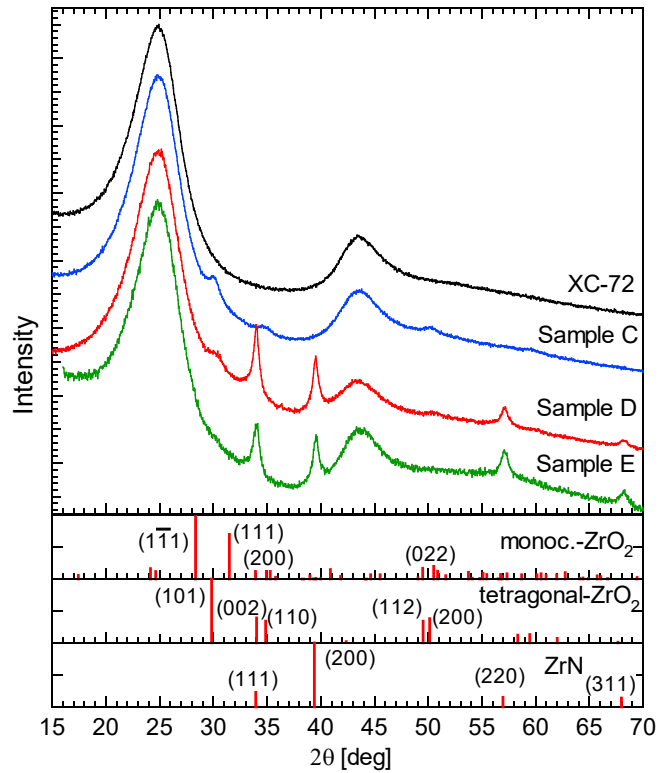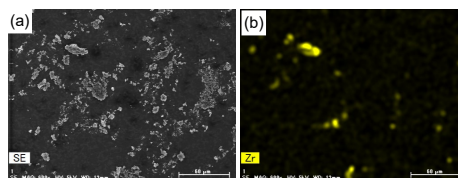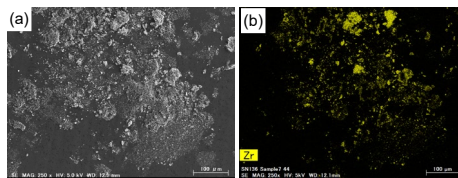
Fig.3 Powder XRD diagrams of XC-72 particles and
samples C, D and E deposited on XC-72.

Figs.4 (a) SEM image and (b) Zr distribution
measured by EDS of sample E.

Figs.5 (a) SEM image and (b) Zr distribution
measured by EDS of sample F.

C. *Film deposition on CGB-10 particles*

Samples G and H were deposited on CGB-10, which has a larger particle size than XC-72 and exhibits a shape close to a sphere, under the same conditions as samples E and F, respectively. The SEM images and EDS mapping of sample G and H shown in Figs. 6(a) and 6(b) indicated that CGB-10 particles kept good dispersity after film deposition. The comparison of EDS images of Figs. 6 showed that the entire surface of almost all CGB-10 particles deposited under vibration (Sample H) was covered with deposited Zr even though differences in the degree of deposition was observed. The Zr distribution was largely different depending on the shape and size of the fine particles, XC-72 and CGB-10. Each CGB-10 particle is closer to spherical and more monodispersive than XC-72 one, so that CGB-10 particles were susceptible to the vibrating equipment resulting in film deposition over the entire surface of the particle.
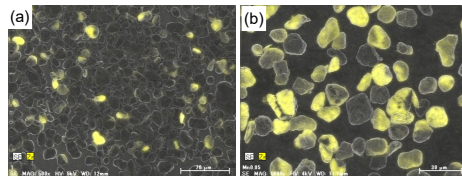
Figs.6 SEM image and Zr distribution measured
by EDS of (a) sample G and (b) sample H.

The X-ray diffraction of sample H shown in Fig. 7 indicated the diffraction peaks at 28.3°, 31.5° and 30.2° assigned to monoclinic and tetragonal ZrO_2, even though baking for the particle was carried out before sputtering. This assumed to be due to CGB-10 having a graphite structure unlike XC-72 which is a carbon black. It is possible that the oxygen contained in CGB-10 powder is not only adsorbed oxygen on the surface of the

particles, but also chemically bound between layers of graphite, and that the heater system used in this study was unable to remove the oxygen. To remove such oxygen, CGB-10 powder was heated in a microwave oven at 500 W for 5 min before being placed in the vacuum chamber. Sample I was deposited on microwaved CGB-10 under the same conditions as sample H. The XRD diagram of sample I shown in Fig. 7 indicates that the peaks at 28.3°, 31.5° and 30.2° can be assigned to monoclinic and tetragonal ZrO_2 decreased in intensity and peaks at 33.9° and 39.4° assigned to ZrN were clearly observed. These indicated that the irradiation by microwave is effective in removing oxygen adsorbed chemically on CGB-10 particles. Figure 7 shows the X-ray diffraction patterns of Samples J-M deposited under the same conditions as sample I except with oxygen flowing, at a gas flow at a rate of 0.2 – 0.8 sccm during film deposition. In Sample J deposited with an oxygen flow at a rate of 0.2 sccm, the diffraction peaks at 33.9° and 39.4° assigned to ZrN become weak in intensity and the diffraction peak at about 30.3° assigned to ZrON phase become intense. The diffraction peaks of Zr_2ON_2, $Zr_7O_8N_4$ and tetragonal ZrO_2 are quite similar to each other because of reflecting their similar atomic arrangement in crystals but can be distinguished from the fact that the main diffraction peak at around 31° shifts to a lower angle with increase in fraction of oxygen in the crystals. The main diffraction peak of Zr_2ON_2 with low fraction of oxygen can be observed at a higher angle than $Zr_7O_8N_4$ with high fraction of oxygen. The deposited film of Sample J is mainly composed of Zr_2ON_2, while in Samples K and L deposited under oxygen flow at a rate of 0.4 and 0.6 sccm, respectively, main precipitated crystalline phase was $Zr_7O_8N_4$ with higher oxygen fraction. The presence and intensity change of the diffraction peaks at 28.3° and 31.5° indicated that monoclinic ZrO_2 was

precipitated in Sample L deposited under oxygen flow at a rate of 0.6 sccm and increases with increase in oxygen flow rate. After removing adsorbed oxygen from carbon particles, ZrON crystals with desired nitrogen to oxygen ratio could be formed on the surface of fine carbon particles by changing the oxygen flow rate from 0 to 0.8 sccm.
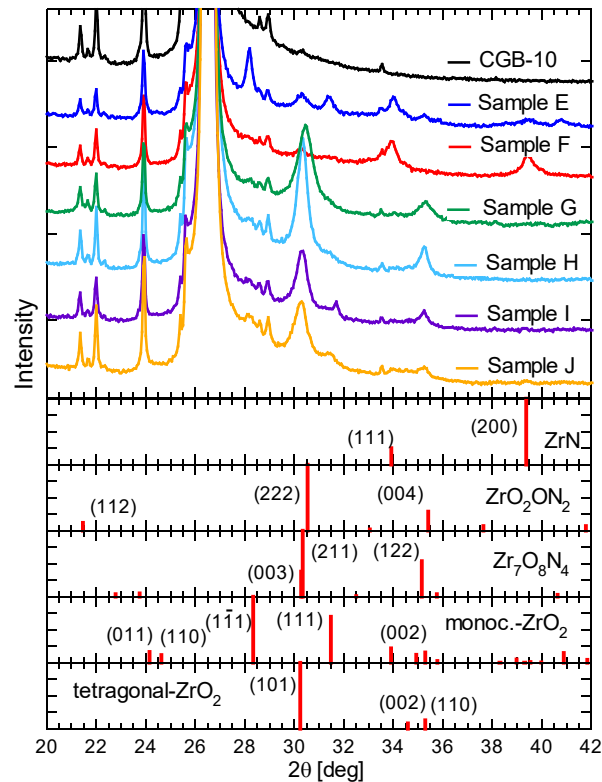

Fig.7 Powder XRD diagrams of CGB-10 powder and samples H to M deposited on CGB-10.

D. *Electrochemical measurement*

Electrochemical measurement was performed on MEAs made from Samples I~M and working electrode potential dependence curve for current density of ORR, I_{ORR}, obtained from SSV measurements were shown in Fig. 8. It is believed that the crystalline phase of catalyst dominates onset potential for ORR. The onset potential for ORR, E_{ORR},

increased to 0.38 V with increase in oxygen flow rate up to 0.6 sccm (MEAs made from sample J, K and L) following decrease for MEA made from sample N. The current density of ORR will be proportional to effective area of catalyst for ORR. MEA made from sample L deposited under oxygen flow at a rate of 0.6 sccm has the largest oxygen reduction current at a working electrode potential of -0.10 V, which is -240 $\mu A/cm^2$, and the oxygen reduction current also decreased with increase or decrease in oxygen flow rate during film formation, as shown in the inset of Fig. 8. This change in ORR depending on oxygen flow rate is consistent with the results of previous study,[21] in which thin films composed of ZrON crystals were deposited on carbon plate substrates in our laboratory. It was confirmed that Zr_2ON_2 and $Zr_7O_8N_4$ make a particularly large contribution to ORR as a catalyst. The I_{ORR} of MEA made from sample L deposited on CGB-10 particles at an oxygen flow at a rate of 0.6 sccm evaluated -240 $\mu A/cm^2$ at applied potential of -0.10 V. In contrast, the I_{ORR} of thin film deposited on the PFC plate substrate shown by dotted curve in Fig. 8 evaluated around -74 $\mu A/cm^2$. The surface area of CGB-10 particles in a unit area of MEA film can be roughly estimated to be around 10 times higher than MEA film based on the mass of the MEA film and CGB-10 particles, and the specific surface area of CGB-10 particles. It was found that the I_{ORR} of the MEA made from the film-deposited particles was higher than that of the film deposited on carbon plate substrate, but not as high as expected. It is believed that the quality of the deposited film on carbon particles should be improved by increase in film thickness, crystallinity and uniformity, and the current density would be increased to be even closer to the actual surface area ratio.
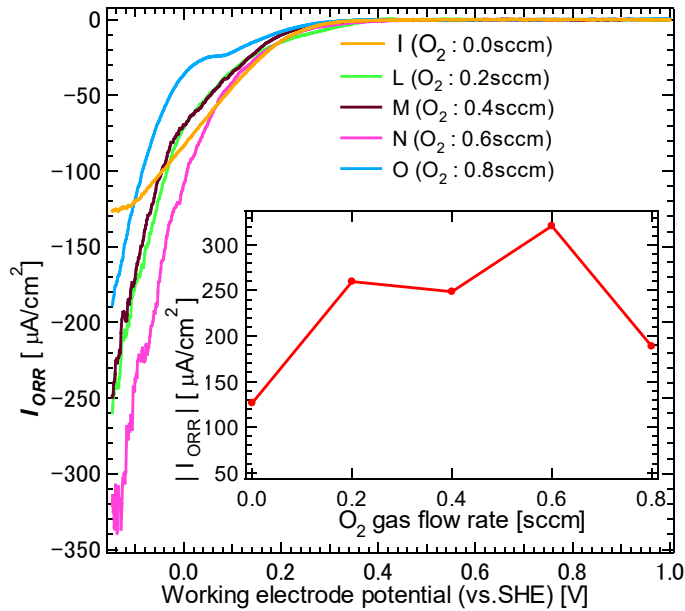
Fig. 8 SSV measurement of sample I to M and thin film deposited on the PFC plate substrate (shown by dotted curve).

IV. CONCLUSIONS

The vibrating equipment with heating capability was developed and introduced to our magnetron sputtering apparatus with a Zr hollow cylindrical target. For the film deposition on spherical alumina particles with high monodispersity, the vibrating equipment was quite effective to uniform deposition over the entire surface. In the deposition on XC-72, a polycrystallised pure ZrN thin film was obtained by baking the particles to remove adsorbed oxygen and then depositing the film while heating. However, after the film deposition on XC-72 particles, some of the particles agglomerated and the deposited Zr was ubiquitous on the agglomerated particles. The CGB-10 particles are different in specification from the XC-72 particles and have

relatively high monodispersibility, so the vibrating equipment was effective in depositing films on the entire surface. Oxygen adsorbed on CGB-10 can be removed by microwave irradiation, and thin films of desired composition can be obtained by changing oxygen flow rate. Electrochemical measurements revealed that MEA made from deposited carbon particles increased in current density for ORR compared to the thin film deposited on carbon plate substrate, but not as high as expected by estimation based on surface area.

ACKNOWLEDGMENTS

Conflict of interest

The authors have no conflicts to disclose." For more information

DATA AVAILABILITY

The data that support the findings of this study are available from the corresponding author upon reasonable request.

REFERENCES

[1]T. Ito, U. Matsuwaki, Y. Otsuka, M. hatta, K. Hayakawa, K. Matsutani, T. Tada and H. Jinnai, Electrochemistry **79**, 374 (2011).

[2]C. Sealy, Mater. today **12,** 65 (2008).

[3]H. M. Barkholtz, L. Chong, Z. B. Kaiser, T. Xu and D.-J. Liu, Int. J. Hydrogen Energy **41**, 22598 (2016).

[4]A. Serov, M. J. Workman, K. Artyushkova, P. Atanassov, G. McCool, S. McKinney, H. Romero, B. Halevi and T. Stephenson, J. Power Sources **327**, 557 (2016).

[5]T. Reshetenko, A. Serov, M. Odgaard, G. Randolf, L. Osmieri and A. Kulikovsky, Electrochem. Commun. **118**, 106795 (2020).

[6]X. Yang, F. Zhao, Y.-W. Yeh, R.S. Selinsky, Z. Chen, N. Yao, C.G. Tully, Y. Ju and B. E. Koel, Nat. Commun. **10**, 1543 (2019).

[7]M. Chisaka, T. Iijima, T. Yaguchi and Y. Sakurai, Electrochim. Acta **56**, 4581 (2011).

[8]P. Chandran, A. Ghosh and S. Ramaprabhu, Sci. Rep. **8**, 3591 (2018).

[9]J. Y. Kim, T-K. Oh, Y. Shin, J. Bonnet and K. S. Weil, Int. J. Hydrogen Energy **36**, 4557 (2010).

[10]A. Ishihara, M. Tamura, Y. Ohgi, M. Matsumoto, K. Matsuzawa, S. Mitsushima, H. Imai and K. Ota, J. Phys. Chem. C **117**, 18837 (2013).

[11]F. Yin, K. Takanabe, J. Kubota and K. Domen, J. Electrochem. Soc. **157**, B240 (2010).

[12]M. Chisaka, A. Ishihara, K. Ota and H. Muramoto, Electrochim. Acta **113**, 735 (2013).

[13]G. Wu, K.L. More, C. M. Johnston and P. Zelenay, Science **332**, 443 (2011).

[14]M. Chisaka, A. Ishihara, H. Morioka, T. Nagai, S. Yin, Y. Ohgi, K. Matsuzawa, S. Mitsushima and K. Ota, ACS Omega **2**, 678 (2017).

[15]G. Liu, H. M. Zhang, M. R. Wang, H. X. Zhonga, and J. Chen, J. Power Sources **172**, 503 (2007).

[16]Y. Yuan, J. Wang, S. Adimi, H. Shen, T. Thomas, R. Ma, J. P. Attfield and M. Yang, Nat. Mater., **19**, 282 (2020).

[17]Y. Ohgi, A. Ishihara, K. Matsuzawa, S. Mitsushima, K. Ota, M. Matsumoto, and H. Imai, ECS Transactions **33**, 609 (2010).

[18]X.-Z. Wang, H. Luo, T. Muneshwar, H.-Q. Fan, K. Cadien and J.-L. Luo, ACS Appl. Mater. Inter. **10**, 40111 (2018).

[19]A. S. Kuprin, A. Gilewicz, T. A. Kuznetsova, V. A. Lapitskaya, G. N. Tolmachova, B. Warcholinski, S. M. Aizikovich and E. V. Sadyrin, Materials **14**, 1483 (2021).

[20]A. Ishihara, J.-H. Kim, Y. Maekawa, S. Mitsushima, and K. Ota, J. Hydrog. Energy Syst. Soc. Jpn. **33**, 38 (2008).

[21]H. Iwata, H. Ishii, D. Kato, S. Kawashima, K. Kodama, M. Furusawa, M. Tanaka and

T. Sekiya, J. Vac. Sci. Tech. A **36**, 061509 (2018).

[22]B. Fu and L. Gao, J. Am. Ceram. Soc. **87**, 696 (2004).

[23]P. Carvalho, J. M. Chappé, L. Cunha, S. Lanceros-Méndez, P. Alpuim, F. Vaz, E. Alves,

C. RousselotJ. P. Espinós, and A. R. González-Elipe, J. Appl. Phys. **103**, 104907

(2008).